High Temperature Interaction Behavior at Liquid Metal-Ceramic Interfaces

S.M. McDeavitt, G.W. Billings, and J.E. Indacochea

(Submitted 25 February 2002; in revised form 2 April 2002)

Liquid metal/ceramic interaction experiments were undertaken at elevated temperatures with the purpose of developing reusable crucibles for melting reactive metals. The metals used in this work included zirconium (Zr), Zr-8 wt.% stainless steel, and stainless steel containing 15 wt.% Zr. The ceramic substrates include yttria, Zr carbide, and hafnium (Hf) carbide. The metal-ceramic samples were placed on top of a tungsten (W) dish. These experiments were conducted with the temperature increasing at a controlled rate until reaching set points above 2000 °C; the systems were held at the peak temperature for about five min and then cooled. The atmosphere in the furnace was argon (Ar). An outside video recording system was used to monitor the changes on heating up and cooling down. All samples underwent a post-test metallurgical examination. Pure Zr was found to react with yttria, resulting in oxygen (O) evolution at the liquid metal-ceramic interface. In addition, dissolved O was observed in the as-cooled Zr metal. Yttrium (Y) was also present in the Zr metal, but it had segregated to the grain boundaries on cooling. Despite the normal expectations for reactive wetting, no transition interface was developed, but the Zr metal was tightly bound to yttria ceramic. Similar reactions occurred between the yttria and the Zr-stainless steel alloys. Two other ceramic samples were Zr carbide and Hf carbide; both carbide substrates were wetted readily by the molten Zr, which flowed easily to the sides of the substrates. The molten Zr caused a very limited dissolution of the Zr carbide, and it reacted more strongly with the Hf carbide. These reactive wetting results are relevant to the design of interfaces and the development of reactive filler metals for the fabrication of high temperature components through metal-ceramic joining. Parameters that have a marked impact on this interface reaction include the thermodynamic stability of the substrate, the properties of the modified interface, the temperature-dependent solubility limits of the liquids and solid phases, and the high-temperature stoichiometry of the ceramic.

Keywords liquid metal/ceramic interface, reactive wetting, Yttria substrate, Zirconium and Hafnium Carbide substrates, zirconium metal, zirconium-stainless steel alloys

I. Introduction

Several industrial applications require advanced materials that will endure hostile chemical environments and more demanding thermal and mechanical conditions. In most cases, no unique class of materials can sustain these challenging conditions.[1] For instance, the need to improve the thermal efficiency of automotive engines demands higher operating temperatures, which in turn require materials with high temperature strength and resistance to corrosion and wear. Engineering ceramics may be the materials of choice based on the design requirements, but their brittle nature, poor machining properties, intricate technical designs, and cost severely limit their widespread utilization as monolithic components. On the other hand, their use can be expanded if the nonmetallic materials can be joined to metals or as ceramic-metal composite components. For example, high-temperature turbines require ceramic coatings on the metal to protect them from oxidation and erosion. Combined metal and ceramic materials are also used in the electronics industry as hybrid ceramic circuits.

Assembling a ceramic-metal composite is complicated because of the weak link between the dissimilar materials. Nearly all ceramic-metal couples exhibit a large coefficient of thermal expansion mismatch, which leads to large thermal stresses during cooling from the fabrication temperature[2,3] or from thermal cycling in service. In general, these stresses must be relieved by the plastic deformation of the metallic phase, or cracks can develop at the ceramic-metal interface or in the ceramic near the interface.[4-6] Ideally, a ductile metal (e.g., copper (Cu) or aluminum (Al)) can be used to deform and relieve these thermal stresses, but most ductile metals do not wet ceramics.

The basic cause of ceramic non-wettability is the unusually nonmetallic bonding (ionic or covalent) of their lattices and consequent lack of delocalized binding electrons needed to continue a metallic condition and, hence, create a ceramic-metal interface of low surface energy. The energy of such an interface is usually larger than that of the ceramic substrate. To achieve the necessary decrease in surface energy, the chemistry of the interface must be changed. The exposure of a ceramic surface to a reactive metal results in the reduction of the ceramic phase and formation of new phases at the ceramic-metal interface.[7-10] Reaction product sequences can become com-

S.M. McDeavitt, Argonne National Laboratory, Chemical Technology Division, Argonne, Illinois 60439; **G.W. Billings,** West CERAC, Inc., McCarran, Nevada 89434; and **J.E. Indacochea,** University of Illinois at Chicago, CME Department, Chicago, Illinois 60607. Contact e-mail: mcdeavitt@cmt.anl.gov.

plex, and the resulting structure is often an elaborate series of interfacial product layers. The thickness and mechanical properties of each phase, the thermal expansion mismatch, and adhesion at each interface play significant roles in the final properties of the joint or composite structures.[5,8] Thus, it can be said that the performances of systems that include ceramic-metal interfaces are governed by the interface morphology and stability.

The interaction studies reported here were performed while screening materials for advanced multi-use crucibles for processing Zr alloys at 1600 °C. This particular application requires non-wetting properties, which is the exact opposite of the required behavior for joining and brazing. While our first application was to identify non-wetting liquid metal-ceramics combinations, the resulting database is full of metal-ceramic interfaces developed through reactive wetting. The metal-ceramic combinations highlighted below include high purity Zr and Zr alloys (i.e., stainless steel-15 wt.% Zr and Zr-8 wt.% stainless steel) in contact with Y oxide, Zr carbide, and Hf carbide. This particular spectrum of materials illustrates interfaces that may develop during reactive wetting for causes where extensive metal-ceramic chemical interaction is not observed.

2. Experimental Procedure

The high-temperature experiments consisted in placing small solid metal specimens onto ceramic substrates. A variety of ceramics (including yttria, Zr nitride, Zr carbide, and Hf carbide) were fabricated from high-purity powders (99.9% purity) by hot uniaxial compression pressing (HUP). All samples were cleaned carefully to remove surface contaminants using acetone, and then dried totally before placing them in the furnace. The metal specimens included pure Zr (99.5% pure with Hf, C, Cr, and Fe as contaminants), Zr + 8 wt.% stainless steel, and stainless steel alloyed with 15 wt.% Zr. The composition of the stainless steel (HT-9), in weight percent, is 0.5 Ni, 12.0 Cr, 0.2 Mn, 1.0 Mo, 0.25 Si, 0.5 W, 0.5 V, 0.2 C, and balance Fe. The metal-ceramic arrangement was heated in a tungsten mesh furnace in high-purity Ar gas (research grade, 99.99% purity); a sensing thermocouple was placed approximately 0.5 cm beneath the samples. The materials were preheated to 600 °C, continuously heated at a rate of about 20 °C/min-1600 °C, and then at 10 °C/min-2000 °C. In most cases, the peak temperature was held for 5 min and then cooled at ~200 °C/min-1200 °C, followed by an uncontrolled cooling to room temperature. The changes of the solid metal during heating leading to their melting, the wetting of the ceramic substrate, and high-temperature interactions between the molten metals and ceramic substrates were monitored through an external video camera. The in situ observations were followed by post-test examinations using scanning electron microscopy (SEM) and energy dispersive spectroscopy (EDS).

3. Results and Discussion

3.1 Zr-Y_2O_3 System

The Zr sample melted at ~1850 °C, and immediately wetted the Y_2O_3 (a contact angle of ~50° was measured). No reactions were observed at the interface before melting, though some reactions were detected as the molten Zr was in contact with the yttria. Liquid bubbling at the interface was observed in the video, which gives evidence of some sort of chemical reactions. The chemical reaction that is most likely to occur, based on the components of the system as well as the compositional and metallurgical changes experienced by the original Zr metal, is the reduction of Y_2O_3 by the Zr:

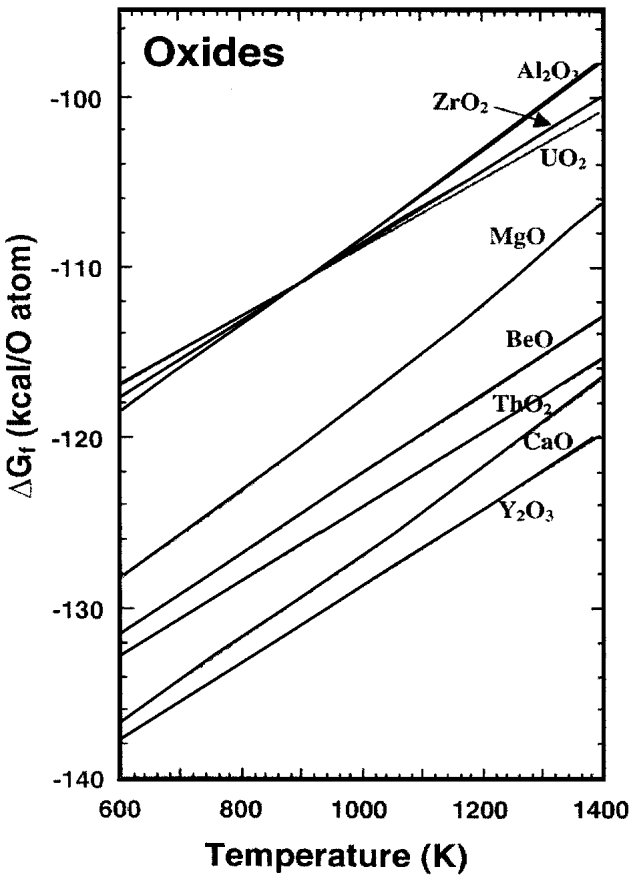

Fig. 1 Standard free energies of formation of selected oxides as function of temperature (calculated)

$$Y_2O_3 + 3Zr \rightarrow 3\ Zr(O) + 2Y_{[Zr(O)]}. \quad \text{(Eq 1)}$$

According to equilibrium thermodynamics, ZrO_2 is unlikely to form in this reaction since Y_2O_3 is more stable based on the energies of formation of these oxides, as shown in Fig. 1. In addition, no transition phase formed between the Zr-metal and the ceramic substrate, a likely location for the ZrO_2 if it were to form. Both O and Y are expected to diffuse to and dissolve in the molten Zr; this is anticipated from examining the Zr-O and Y-Zr equilibrium phase diagrams in Fig. 2.[11]

A light gray band, ~25 μm thick, was observed at the Zr-Y_2O_3 interface, which was found to contain higher amounts of oxygen relatively to the bulk of the solidified and now a Zr-alloy (Fig. 1). The dark precipitate at the grain boundaries of the Zr metal contains Y, which was determined by EDS analysis. The segregation of Y to the grain boundaries is caused by its lower solubility in α-Zr, as noted in Fig. 3(b). The oxygen

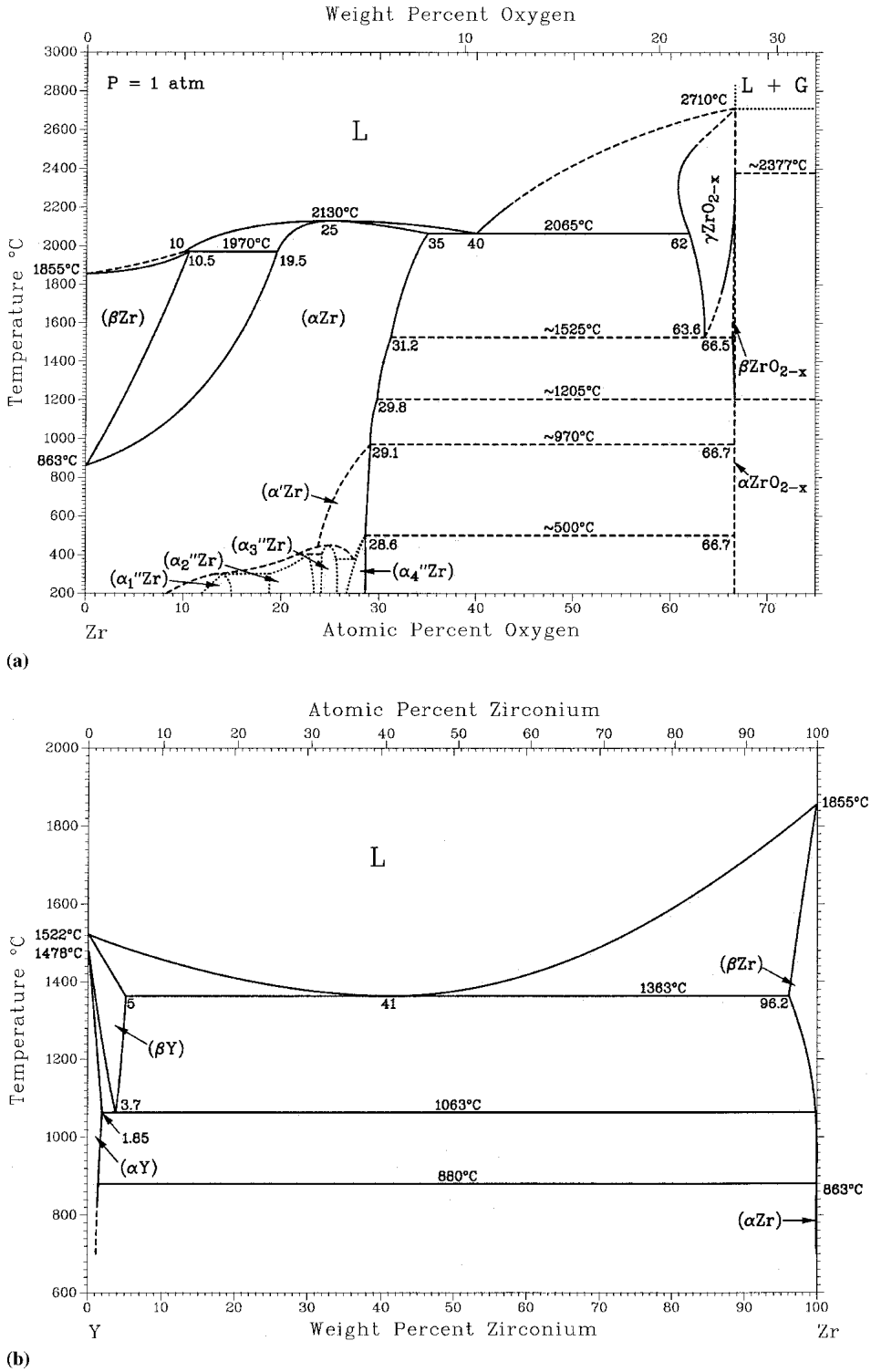

Fig. 2 Equilibrium phase diagrams for **(a)** Zr and O and **(b)** Y and Zr[11]

enrichment of the Zr at the interface is likely caused by its proximity to the oxide ceramic, where the Y_2O_3 was locally reduced.

The roughness of the ceramic substrate at the interface is evidence of the partial dissolution of its surface as it reacted with the molten Zr. There was a continuous transition from the solidified Zr metal into the Y_2O_3 without any transition phase or precipitate at this interface, as observed in Fig. 4. The solidified metal droplet was tightly bonded to the ceramic substrate. Cracking in the ceramic was observed near the interface (Fig. 3) because of differences in thermal expansion coefficients between Zr and Y_2O_3.

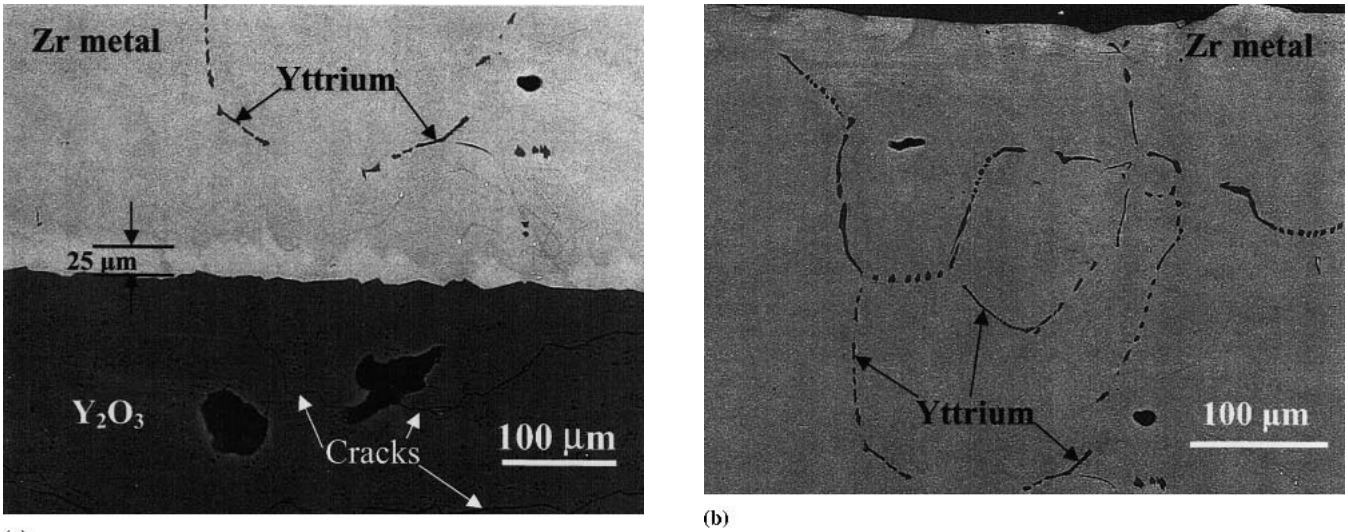

Fig. 3 SEM micrographs of **(a)** Zr/Y_2O_3 interface with cracks in Y_2O_3 and **(b)** segregation of Y to the Zr-metal grain boundaries

3.2 Stainless Steel-15 wt.% Zr/Y_2O_3 System

This alloy melted completely at ~1350 °C, which is near the eutectic temperature for Fe-15 wt.% Zr alloy, which is ~1337 °C.[12] The liquid metal did not wet the ceramic immediately after melting. The contact angle was measured initially as ~110°, and it varied unexpectedly with increasing temperature; these changes in wetting angle are shown in Table 1. The changes in the contact angle may be attributed to the chemical reactions occurring at the interface, which affect the localized composition of the alloy and hence it would also influence the wetting angle. The system was held at the peak temperature for 5 min, where the contact angle became 60°; it was then cooled at a controlled rate to 1200 °C, where the furnace was shut down and the system allowed to cool to room temperature. No reactions were evident in the video as the temperature increased from 1530-2000 °C; it is likely that the lower melting temperature of the alloy could have covered possible reactions that may have occurred between the metal alloy and the Y_2O_3 substrate.

The metal droplet bonded to the Y_2O_3, but a gap is observed between the solidified Zr and the ceramic substrate, as seen in Fig. 5(a) and (b). Extensive cracking was also observed in the Y_2O_3 substrate adjacent to the interface; this implies that a bonding developed across metal/ceramic system and the cracking, as well as the separation of the metal bead from the Y_2O_3, was caused by the difference in their coefficients of thermal expansion. Unlike the pure Zr/Y_2O_3 system, a transition or reaction layer was formed at the metal side of the interface in this system, as seen in Fig. 5(b). This reaction layer was very thin and not uniform in thickness, which may explain why the metal separated from the ceramic easily. EDS spot analysis of this layer at three different locations gave a composition in weight percent of 80.0-85.0 Zr, 11.5-13.0 Y, 2.4-2.8 Fe, 1.0-1.3 Ni, and small amounts of Cr and Si. The light gray areas of the stainless steel alloy (Fig. 5b) have a composition in weight percent of 57.5 Fe, 36.0 Zr, 4.5 Cr, 1.0 Ni, and Si. The EDS spot analysis of the dark gray areas gave the following chemistry (wt.%): 85.0 Fe, 14.0 Cr, 0.8 Ni, and Si. It can be seen from these chemical analyses that yttrium was confined to the interface, and the reaction layer; the level of Zr was also higher at the reaction layer.

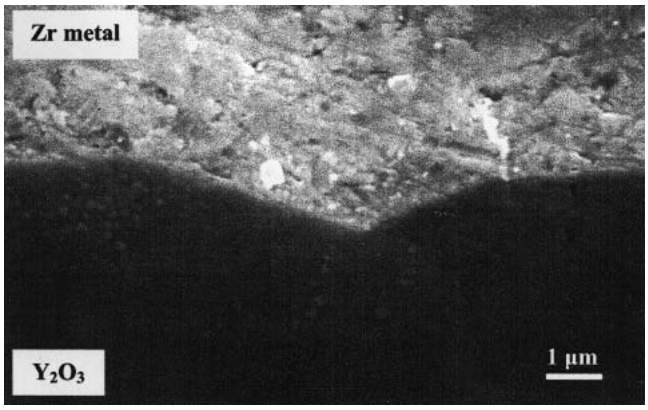

Fig. 4 Interface between Zr-metal and Y_2O_3 after the thermal cycle. There is strong bonding and continuity at the interface.

Table 1 Changes in the Contact Angle With Increasing Temperature in the SS-15 wt.% Zr/Y_2O_3 System

Temperature, °C	Contact Angle, °
1350	110
1370	95
1780	115
1950	140
>2000	90, 60

3.3 Zr -8 wt.% Stainless Steel /Y_2O_3 System

The type of interface activity between the Zr-8SS alloy and Y_2O_3 was similar to that of the pure Zr and Y_2O_3; bubbling was observed at the liquid-ceramic interface occurred at ~1850 °C. At ~1870 °C the metal alloy melted entirely and wetted the Y_2O_3; a contact angle between 35° and 40° was measured. A

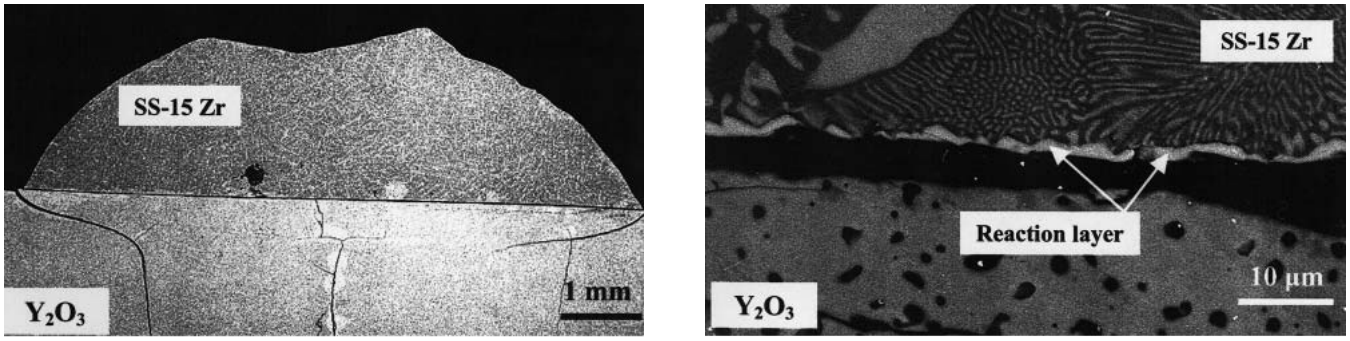

Fig. 5 Micrographs of the SS-15 Zr/Y_2O_3 system showing **(a)** wetting characteristics of the solid metal droplet and cracking of the Y_2O_3 and **(b)** interfacial gap and the reaction layer on the metal side of the interface

light gray region 10-20 μm thick was also observed in the Zr metal by the interface (Fig. 6a). An interface scan using wavelength dispersion spectroscopy (WDS), as seen in Fig. 6(b), showed O at the interface at ~20 wt.%, and ~12.0 wt.% in the Zr metal. Although no Y was detected at the immediate interface for that particular test spot, this again segregated to the grain boundaries of the Zr-metal, as seen in Fig. 7. Zr was not observed in the ceramic substrate either, as shown by the WDS results. This system, like the pure Zr/Y_2O_3, had no distinct reaction or transition layer, but there was continuity across the interface (Fig. 8) that was apparently enabled by the dissolution of oxygen in the Zr alloy. The metal alloy was strongly bonded to the Y_2O_3, and some cracking was visible at the immediate interface (Fig. 7); the amount of cracking was more than what it was observed between the pure Zr and the Y_2O_3.

3.4 Zr/ZrC System

The Zr metal melted on the ZrC substrate at ~1910 °C, and it flowed extremely and rapidly over the ZrC surface and spilled over to the sides of the ZrC specimen. No chemical reactions were detected in the video before melting. The liquid metal finally rested on the W dish that held the ZrC substrate (Fig. 9a). The molten Zr penetrated between the W holder and the ZrC, and strongly bonded these two materials together, as shown in Fig. 9(b). The top surface of the ZrC (Fig. 9a) remained smooth, with no observable degradation, which may point toward a chemical reaction between the Zr metal and the ZrC. Looking at the thermodynamic data, and particularly at the calculated free energies of formation of selected carbides, shown in Fig. 10, these energies are larger than those of the oxides (Fig. 2) by a factor of 2.5, which may indicate a greater reactivity in the ZrC compared to Y_2O_3. Yet the results show a greater chemical activity between the Zr and the Y_2O_3 than between Zr and ZrC. However, it should be noted that in the Zr/ZrC, a compatible system is expected since the carbide is Zr-based. Review of the Zr-C equilibrium phase diagram,[11] seen in Fig. 11, shows that both α-Zr and β-Zr have limited solubility for carbon (C), but each phase is in equilibrium with ZrC. At higher temperatures, e.g., 2000 °C, the Zr is liquid is expected to be in equilibrium with solid ZrC, as seen in Fig. 11. Furthermore, the phase diagram indicates that the C should not have a significant impact in the melting temperature of Zr, it lowers it to a eutectic temperature of 1806 °C, but in our experiment the alloy melted at about 1910 °C. This discrepancy in the melting temperature might be due to the difficulty of observing the start of melting at the elevated temperature and the position of the thermocouple with respect to the sample that makes it difficult to measure the temperature precisely. The Zr completely wets the ZrC; this can be appreciated at the side of the ZrC (Fig. 9a), where the contact angle between Zr and ZrC is very small.

The unintended, but effective, braze joint between the ZrC substrate and the W metal dish was metallographically studied (Fig. 9b) at a spot corresponding to the circle in Fig. 9(a). Strong bonding was evident between W and ZrC via Zr metal. The interface between the α-Zr and the ZrC is relatively smooth, and it does not show any form of degradation, except for some sporadic cavities. Figure 9(b) shows no transition phase at the interface, but the bonding was strong. The microstructure at this Zr/ZrC interface is consistent with the equilibrium phase diagram (i.e., α-Zr is in equilibrium with ZrC). The very small contact angle between Zr metal and ZrC is further evidence of the compatibility of this system. On the opposite side of the braze metal, the molten Zr reacted with W. According to the Zr-W equilibrium phase diagram,[11] a eutectic appears at Zr-16.6 wt.% W with a melting temperature of about 1735 °C (Fig. 12).

The most likely sequence of events following the melting of Zr and its free flow over the surface of the ZrC is that as the liquid Zr makes contact with the W-dish, underneath the ZrC substrate, it dissolves the W-dish. Since the entire system is held at 2000 °C, this allows time to dissolve enough tungsten that will supersaturate the molten Zr, causing the W_2Zr intermetallic to precipitate. On the other hand, at the surface of the W-dish, Zr will dissolve in the W, forming the intermetallic W_2Zr, which appears as a coating attached to the W in Fig. 9(b). The horizontal discontinuous line included in the phase diagram (Fig. 12) shows the equilibrium phases expected across the W/Zr, which match the phases identified in Fig. 9(b). As the Zr-W liquid alloy drops below 1735 °C, it undergoes a eutectic transformation, whose features are identified in the microstructure. EDS analysis confirmed the composition of the intermetallic phases.

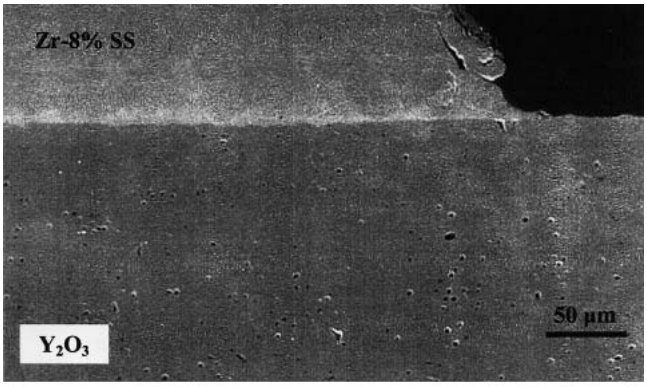

(a)

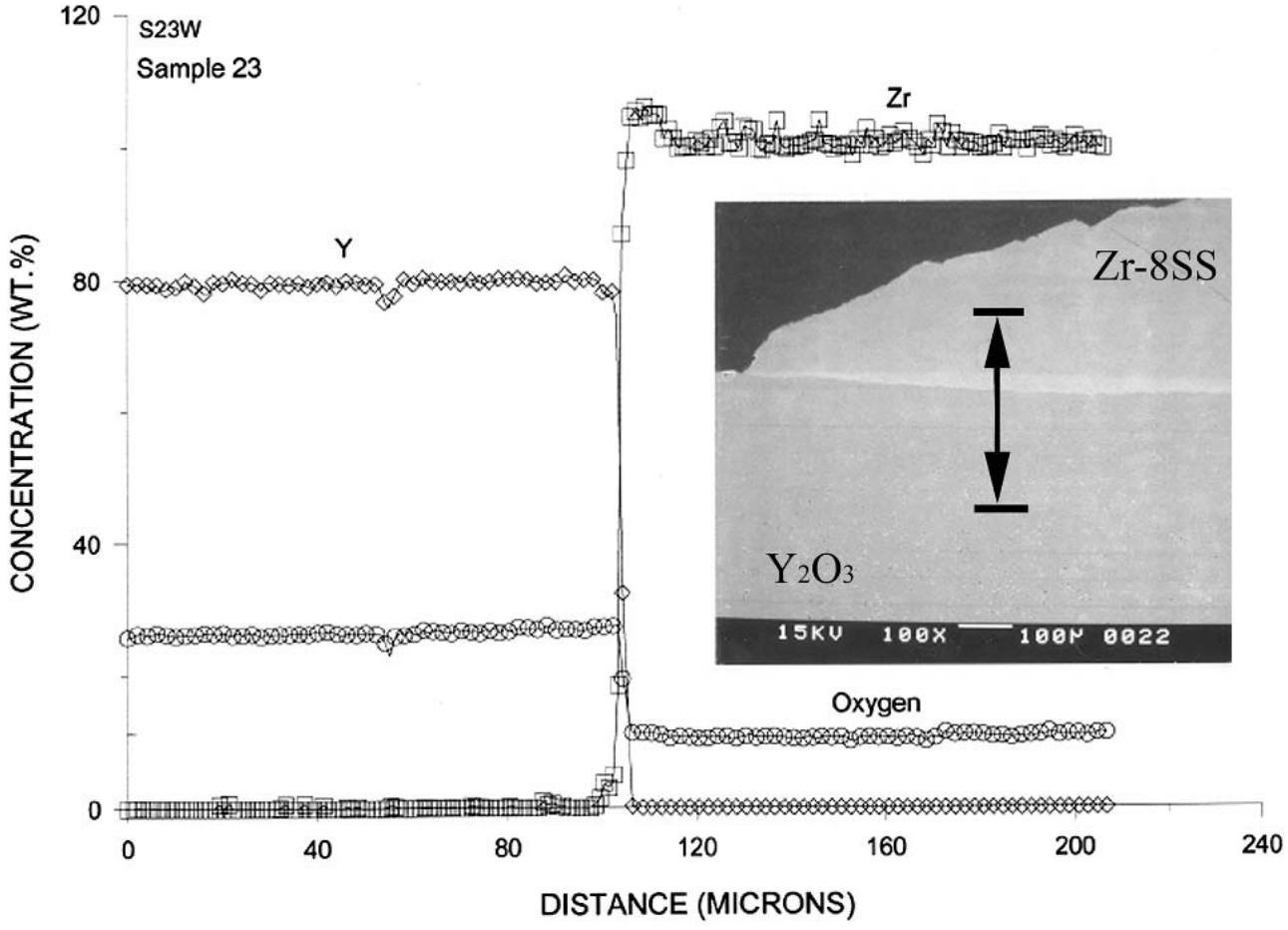

(b)

Fig. 6 **(a)** Micrograph of the Zr-8% SS/Y_2O_3 interface; **(b)** wavelength dispersion spectroscopy results across the interface of the system

3.5 Zr/HfC System

This system behaved similar to the Zr/ZrC system. Zr melted at ~1915 °C, wetted the HfC substrate, and flowed freely over its surface. Most of the liquid metal ended up on the sides of the HfC specimen (Fig. 13a); however a portion of the molten Zr remained on top of the HfC. Some of the molten Zr that rested at the bottom of the W-dish next to the HfC substrate penetrated between the two parts and bonded them together. Although no chemical reaction between Zr and HfC was detected in the video before melting, it was evident in the post-test analysis that some interactions took place between the Zr and the HfC manifested by the microstructure changes in the Zr metal after the thermal cycle. On top surface of the ceramic

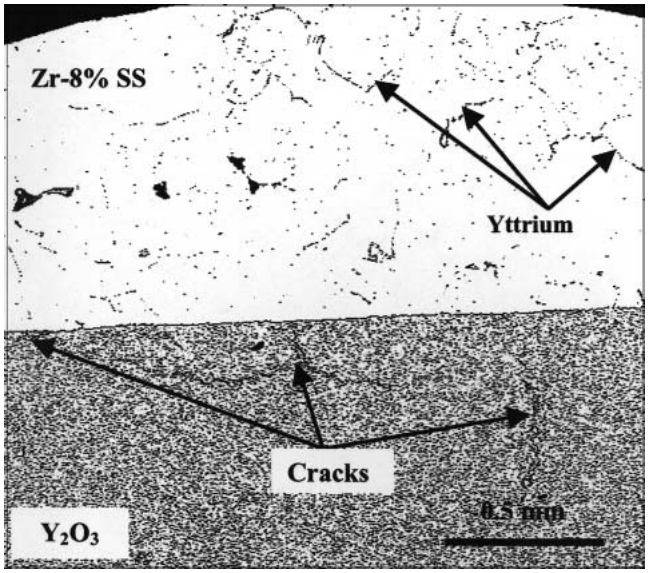

Fig. 7 SEM backscattered micrograph of the Zr-8% SS/Y_2O_3 system. Y segregated to the Zr grain boundaries and cracks were present in the yttria substrate.

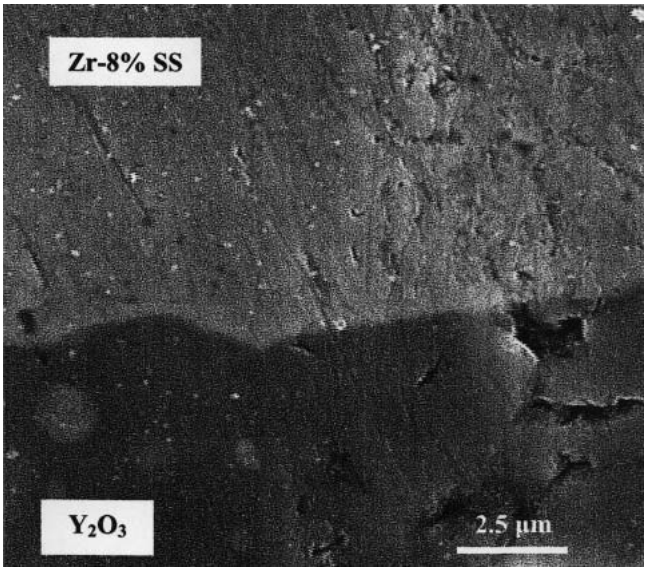

Fig. 8 SEM micrograph of the Zr-8% SS/Y_2O_3 system that shows the solid metal tightly bonded to the yttria and a smooth interface

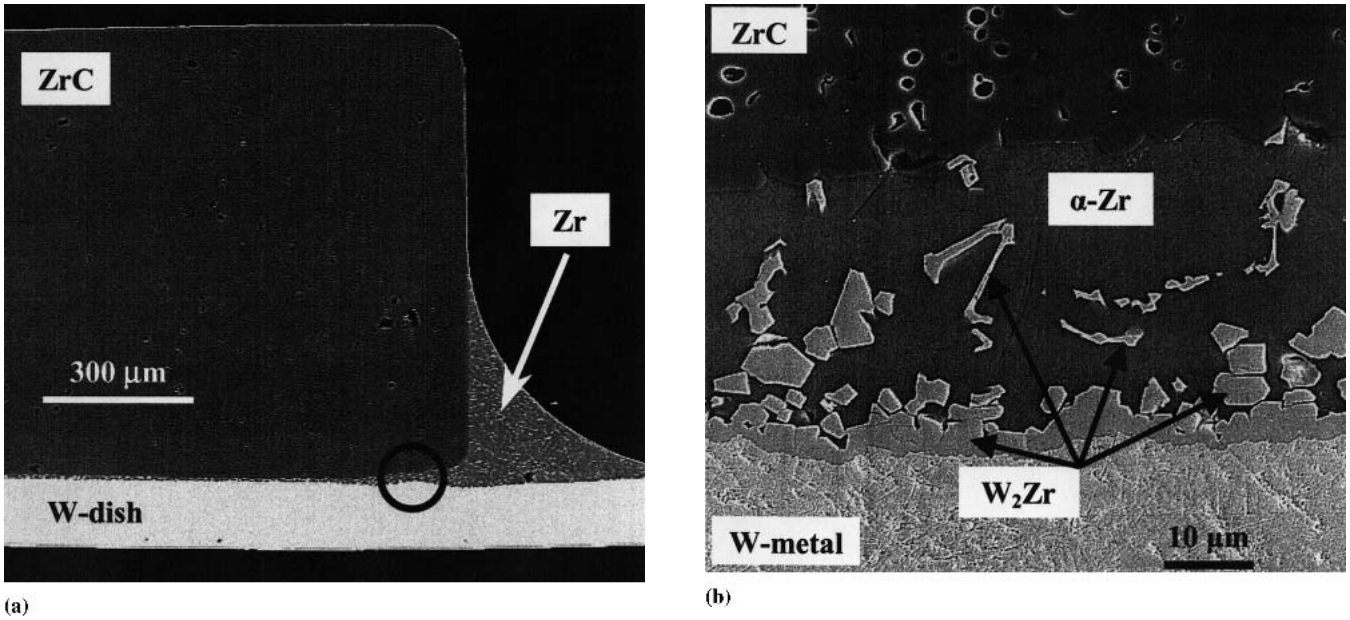

Fig. 9 SEM micrographs of the Zr/ZrC system: **(a)** Molten Zr flowed easily over the ZrC with no chemical interaction. **(b)** Selected "circled area" of (a) that shows a braze joint developed between the ZrC and the W-dish due to the penetration of the molten Zr between them

substrate, Zr dissolved the HfC (Fig. 13b), and HfC grains were pulled away from the substrate. Evidence of the HfC dissolution includes the precipitation of ZrC on the top of the melt as well as the presence of Hf in solid solution (~9-10 wt.% Hf) with the solidified Zr. The precipitated ZrC has a composition of 87 wt.% Zr, 4-6 wt.% Hf and the remaining C. There was no transition reaction layer between the Zr metal and the HfC, but the interface was very rough with significant degradation of the HfC surface. It can be seen that Zr infiltrated along the grain boundaries of the HfC, separating the grains from the bulk of the ceramic substrate.

The increase in the melting temperature of Zr to ~1915 °C suggests the possibility of either a chemical reaction prior to melting or a thermocouple offset. Dissolved Hf will raise the melting point of Zr from 1855 °C, which suggests a local reduction of HfC at the interface. The reduction of HfC by Zr and the formation of ZrC are somewhat unexpected from simple equilibrium thermodynamics, since HfC should be more

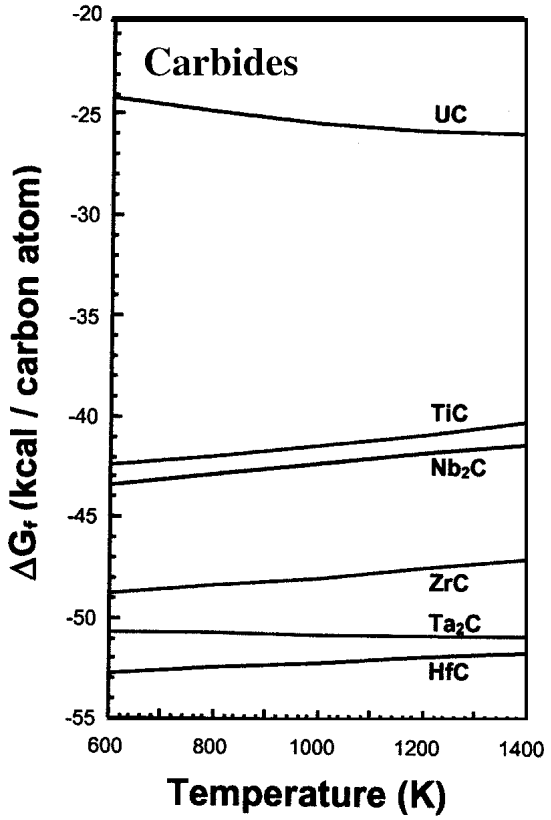

Fig. 10 Standard free energies of formation of selected carbides as function of temperature (calculated)

stable than ZrC according to the energies of formulation shown in Fig. 10. However, the chemical compatibility of Zr and Hf and the perturbations of high temperature thermodynamics may be invoked to provide a plausible first guess toward explaining this observation.

Another location characterized in this system was the interface at the bottom of the HfC with the W-dish, where molten Zr had infiltrated (Fig. 13c). In this area, Zr reacted with both the HfC and the W metal; there was evidence of significant dissolution of W in Zr, which can be noted in Fig. 13(a) at the bottom right hand corner of the HfC resting on the W-dish, where the Zr metal fills that corner. The Zr-W interaction was the same as discussed for the Zr/ZrC system, and obviously the microstructures are very similar between these two systems. That is, a W_2Zr intermetallic-layer transition phase precipitated between the W-metal dish and the infiltrated Zr metal. Most of the intermetallic remained attached to the W dish, but several intermetallic precipitates are imbedded in the Zr metal. In addition, some of the W_2Zr intermetallic was also found in the eutectic structure that exists between W and Zr.

4. Conclusions

Based on the observed results, the following conclusions may be stated:

1. Zr and Zr alloys stimulate reactive wetting with stable oxide and non-oxide ceramics at elevated temperatures. This wetting has implications to the joining of metals and ceramics, especially in cases where the formation of an intermediate reaction zone is minimal.

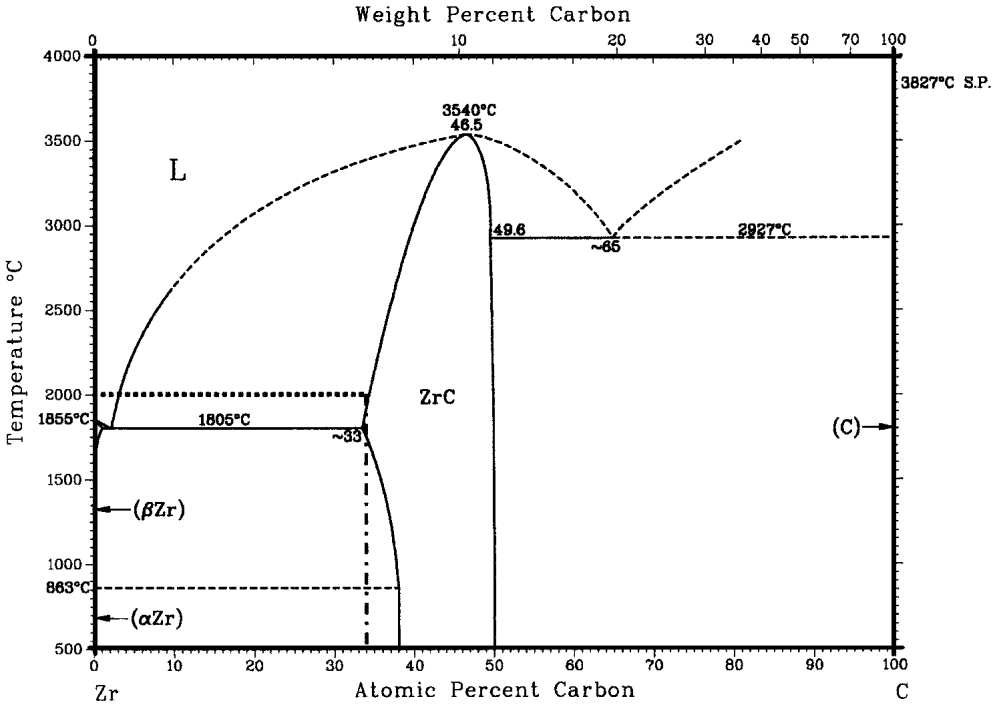

Fig. 11 Equilibrium phase diagram for Zr and C[11]

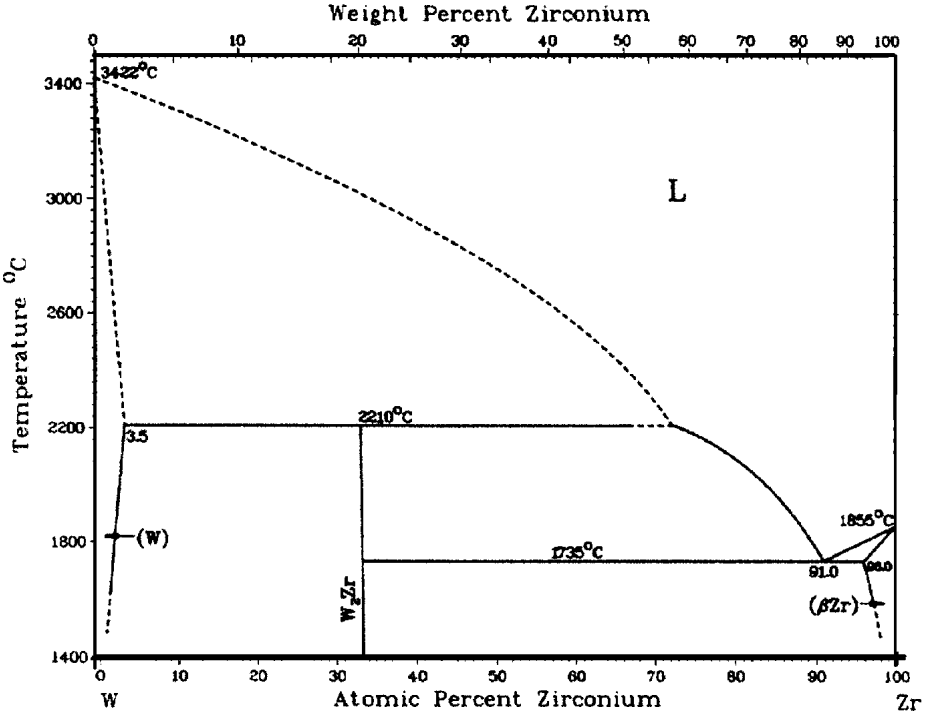

Fig. 12 Equilibrium phase diagram of tungsten and zirconium[11]

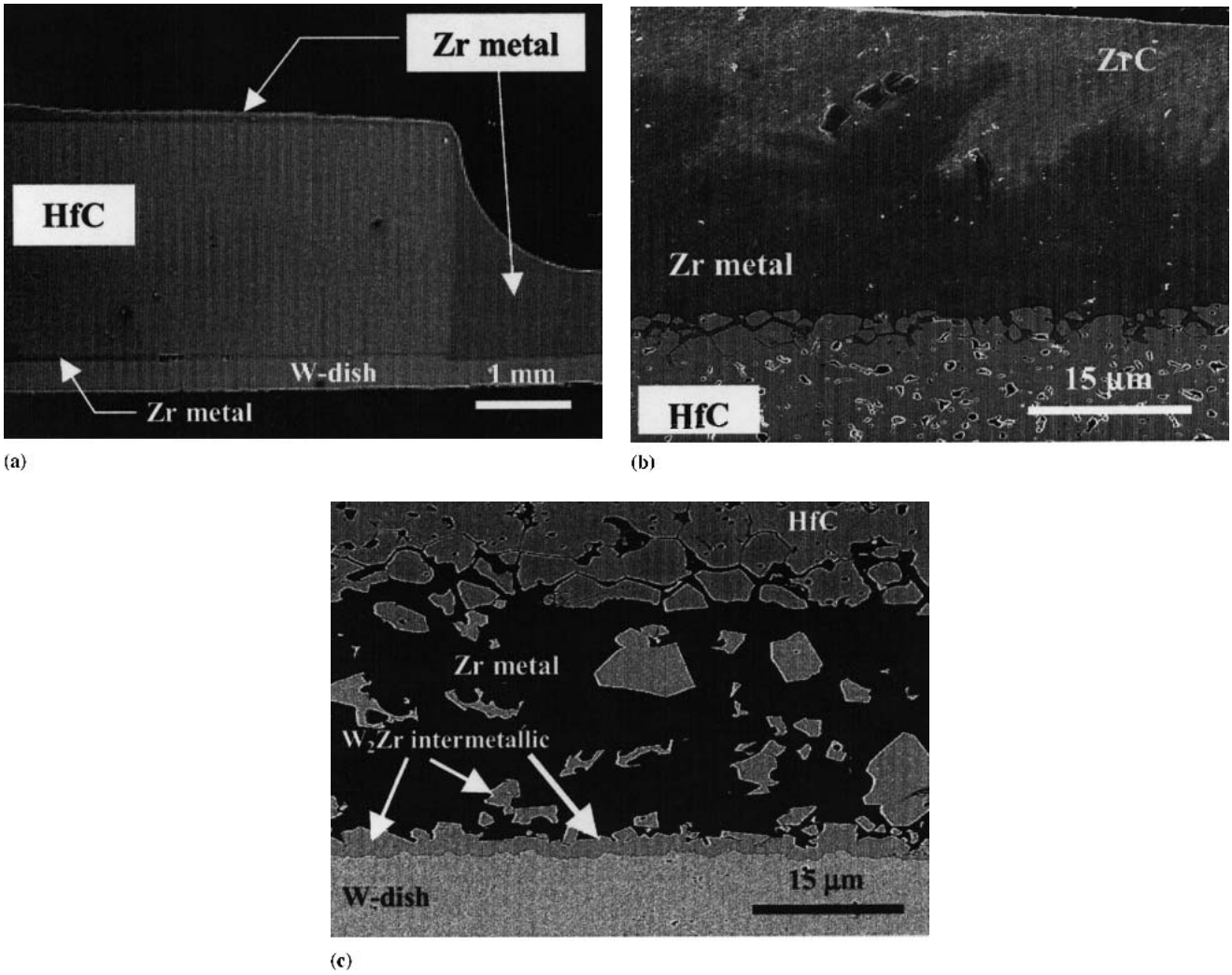

Fig. 13 SEM micrographs depicting microstructural features of the molten Zr/HfC interactions: **(a)** Zr/HfC system with Zr metal present at three locations around the HfC; **(b)** top of the HfC showing dissolution and grain pull out of the HfC and precipitation of ZrC; **(c)** interactions of the Zr metal with the HfC and W-dish at bottom of the ceramic substrate

2. While equilibrium thermodynamics provide a guide to interpret the observed interfacial reactions, it is clear that other parameters are significant at high temperature. These parameters include the properties of the modified interface, the temperature dependant solubility of the liquid and solid phases, and the high-temperature stoichiometry of the ceramic.
3. Interfaces containing metal-ceramic reaction products were observed at the SS-15Zr/Y_2O_3, Zr/ZrN, and Zr/W interfaces, but no transition reaction products were observed across the Zr/Y_2O_3, Zr/ZrC, and Zr/HfC interfaces.
4. This later observation of a continuous and strong bond in Zr/Y_2O_3, Zr/ZrC, and Zr/HfC is contrary to conventional understanding of reactive wetting.

Acknowledgments

The authors would like to acknowledge Dr. L. Leibowitz and Mr. Mark Hash for their review of the manuscript, and the Analytical Chemistry Laboratory of the CMT Division at the Argonne National Laboratory. The U.S. Department of Energy under contract W-31-109-Eng-38 supported this work.

References

1. M.M. Schwartz: *Ceramic Joining,* ASM International, Metals Park, OH, 1990.
2. Y.L. Shen: "Structural Materials Properties, Microstructure and Processing," *J. Mater. Sci. Eng.,* 1998, *A252,* pp. 269-75.
3. S.P. Kovalev, P. Miranzo, and M.I. Osendi: "Finite Element Simulation of Thermal Residual Stresses in Joining Ceramics with Thin Metal Interlayers," *J. Am. Ceram. Soc.,* 1998, *81,* pp. 2342-48.
4. F. Hatakeyama, K. Suganuma, and T. Okamoto: "Solid-State Bonding of Alumina to Austenitic Stainless Steel," *J. Mater. Sci.,* 1986, *21,* pp. 2455-61.
5. A. Bartlet, A.G. Evans, and M. Ruhle: "Residual-Stress Cracking of Metal Ceramic Bonds," *Acta Metall.,* 1991, *39,* pp. 1579-85.
6. A.G. Evans and B.G. Dalgleisch: "The Fracture-Resistance of Metal-Ceramic Interfaces," *J. Mater. Sci. Eng.,* 1993, *A162,* pp. 1-13.
7. A.J. Moorhead and H. Keating: "Direct Brazing of Ceramics for Advanced Heavy Duty Diesels," *Weld J.,* 1986, *65,* pp. 17-31.
8. L. Espie, B. Drevet, and N. Eustathopoulos: "Experimental Study of the Influence of Interfacial Energies and Reactivity on Wetting in Metal-Oxide Systems," *Metall. Trans A,* 1994, *25A,* pp. 599-605.
9. P. Kristalis, B. Drevet, N. Valignat, and N. Eustathopoulos: "Wetting Transitions in Reactive Metal-Oxide Systems," *Scripta Metall.,* 1994, *30,* pp. 1127-32.
10. P. Xiao and B. Derby: "Wetting of Silicon Carbide by Chromium Containing," *Acta Mater.,* 1998, *46,* pp. 3491-99.
11. Anon: *Binary Alloy Phase Diagrams,* 2nd ed., *1-3,* ASM International, Materials Park, OH, 1990.
12. S.M. McDeavitt, D.P. Abraham, and Y.P. Park, "Evaluation of Stainless Steel Zirconium Alloys as High-Level Nuclear Waste Forms," *J. Nucl. Mater.,* 1998, *257*(1), pp. 21-34.